biomass

MDPI

Article

The Impact of Fibre Oxidation on the Preparation of Cellulose Nanocrystals (CNC)

Behzad Ahvazi [1,*], Christophe Danumah [2], Tri-Dung Ngo [2], Zhengxiang Zhu [2] and Heather Lorenz [2]

[1] Canna Stream Solutions Ltd. (CSS), 2500 Stantec Tower, 10220-103 Avenue NW, Edmonton, AB T5J 0K4, Canada
[2] Alberta Innovates-InnoTech Alberta, 250 Karl Clark Road, Edmonton, AB T6N 1E4, Canada
* Correspondence: ahvazi@ualberta.ca

Abstract: This study aimed to evaluate the effect of fibre oxidation on the extent of substituted sulfate on cellulose nanocrystals (CNC). In this investigation, fully bleached softwood (SW) and hardwood (HW) pulps from an Alberta pulp mill were oxidized under low (4%), medium (10%), and the higher-end of medium (14%) oxygen consistencies. The oxidized pulp samples were hydrolyzed with concentrated sulfuric acid under conventional procedures to produce CNC. The CNC materials were then characterized by different qualitative and quantitative techniques to evaluate the effect of oxidations on the number of substituted sulfates and the overall sulfate charge of isolated CNC to develop novel high-value applications. The experimental data show that fibre oxidation helped improve the overall CNC yield, with lower half-ester sulfate contents compared to the controls. The half-ester sulfate contents and the viscosity for SW CNC were found to be higher than their HW CNC counterparts. However, the thermal stability of CNC was found to be better for HW than SW pulps. The emerging data help to prepare and engineer CNC tailored to specific applications.

Keywords: softwood pulp; hardwood pulp; oxidation; cellulose nanocrystals (CNC); sulfate content; characterization

Citation: Ahvazi, B.; Danumah, C.; Ngo, T.-D.; Zhu, Z.; Lorenz, H. The Impact of Fibre Oxidation on the Preparation of Cellulose Nanocrystals (CNC). *Biomass* **2022**, *2*, 316–333. https://doi.org/10.3390/biomass2040021

Academic Editors: Amit K. Jaiswal, Swarna Jaiswal and Bahiru Tsegaye

Received: 26 August 2022
Accepted: 28 October 2022
Published: 2 November 2022

1. Introduction

Modification and characterization of CNC physiochemical properties, especially its surface chemistry, is essential for nanocellulose application development [1–4]. Environmentally friendly routes for modification and processing are of particular interest. Surface functionalization and/or modification may serve different purposes. Still, the formation of stable nanoparticle dispersion in polar/non-polar suspensions or media is a significant step for materials formulation and manufacturing [5]. The dispersion is highly dependent on the CNC stability and its surface charges, mainly attributed to the substituted sulfate groups [1,6–8].

Cellulose is one of the planet's most ubiquitous and abundant polymers [9]. Cellulose is a paracrystalline structural polysaccharide that is present in woody biomass. The basic repeating unit contains two anhydroglucose rings joined via the β-1,4 glycosidic linkages. The cellulose chain has two different OH groups at both ends, showing different behaviors. The C1-OH is an aldehyde group resulting from the ring formation by an intermolecular hemiacetal linkage and has reducing properties, while the OH group at the C4 end of the cellulose chain is an alcoholic hydroxyl with no reducing properties [10–12] as illustrated in Figure 1.

The ability and the extent of sulfate group substitution on the cellulosic backbone are governed by the influence of the non-reducing end groups. Accordingly, there is a need for developing a method of engineering, controlling, and monitoring the reducing ends of polysaccharides before the production of CNC with the desired sulfate contents and surface charges.

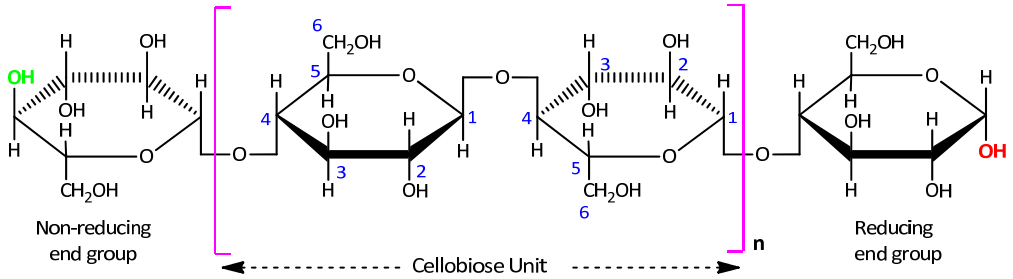

Figure 1. Schematic diagram of the partial molecular structure of cellulose chain with numbering for carbon atoms and **n** = number of cellobiose repeating unit [12].

The hypothesis of this investigation is to modify the reducing end groups in cellulosic fibres by using advanced oxidative degradation processes for controlling the extent of sulfate substitution and the overall surface charges of CNC.

Among a series of oxidation methods [13], oxygen (O_2) and ozone (O_3) are the two most commonly used oxidants that have long been employed in various stages of pulp and paper processing, including the effluent treatment.

The hydrolysis of cellulose-based feedstock using sulfuric acid leads to the production of negatively charged CNC due to the esterification of cellulose hydroxyl groups. However, the extent of sulfate group content and the overall CNC surface charges may hinder the formulation of CNC-based biomaterials, as different CNCs behave differently in hydrophobic media. The inherent polar and hydrophilic nature of CNC challenges their dispersion in organic media and their blending with hydrophobic polymers such as polyethylene (PE), polypropylene (PP), and polystyrene (PS) [5]. CNC's performance and compatibility challenges with other polymers can be addressed by controlling the number of sulfate groups on the surface of CNC and consequently engineering the CNC's overall negative net charge. This strategy allows CNC to be tailored to specific bio-based applications [1–5].

In this study, bleached softwood (SW) and hardwood (HW) kraft pulps were oxidized under three different conditions using oxygen (O_2) oxidation methods. The subsequent oxidized samples were hydrolyzed with concentrated sulfuric acid under a conventional procedure to produce CNC. The CNC materials were characterized by different qualitative and quantitative techniques to evaluate the effect of oxidations on the number of substituted sulfates and the overall surface charges of isolated CNC yields.

Analysis and characterization of the cellulose-based feedstock and their derived CNC materials are essential to reveal pulps and CNCs' features for CNC production process design, improvement, optimization, and application development.

2. Materials and Methods

2.1. Feedstock Furnish

Hardwood kraft (HW) and Softwood kraft (SW) pulps were received as sheets from an Alberta pulp mill. Each was chopped into 10 mm square pieces using a Pierret Chopper and re-pulped with water. Both pin-shredded and re-pulped HW and SW pulps were used for producing different oxidized pulps prior to CNC production at the lab scale at InnoTech Alberta. Pin shredded and re-pulped HW and SW pulps were used as references.

2.2. Oxidation Process

Oxidation of pulp was carried out in a 1-gallon Parr reactor. The pulp sample (100 g) was mixed at the desired consistency (4–14%) with desired NaOH (1–3% O.D. pulp) in a Double Zipper Ziploc plastic bag. Good mixing was achieved by hand-kneading for two minutes. The resulting treated pulp was transferred into a 1-gallon Parr Reactor and mixed at 100 rpm. Once the target temperature (85–100 °C) was reached, the reactor was pressurized to 100 psi with oxygen. The reaction was performed at variable times (50–90 min), and at the end of the reaction, the reactor was depressurized, and the oxidized

pulp was transferred into a white cotton cloth bag. The pulp was washed with RO water and dewatered by a centrifuge to neutralize the pH. The washed oxidized pulps were air-dried before CNC preparation.

2.3. Standard InnoTech Alberta Lab-Scale CNC Production Process

During a standard lab-scale CNC production, approximately 455 g of 63.5 wt% sulfuric acid is added into a 1 L reactor vessel. The solution is heated to 45 °C, and then, approximately 40 g oven-dry mass of cellulosic feedstock (HW, SW, oxidized HW and SW pulps, etc.) is added to the reactor, with the mixture then stirred with an overhead mixer at 200 rpm for 120 min. Once the reaction is completed, the mixture is quenched with RO water (~1500 g) and cooled in an ice bath. Sodium hydroxide (30%) neutralizes the mixture to pH 7 while keeping the temperature below 30 °C under moderate stirring. The neutralized slurry is then centrifuged at 2000 rpm for 10 min to remove clear supernatant, with this step repeated until the entire neutralized sample has been centrifuged. The sediment, consisting of CNC and larger-sized unreacted cellulosic materials, is washed with RO water until its corresponding supernatant reaches a conductivity of ~4 mS/cm and the resulting slurry is then dialyzed using a 6000–8000 Da molecular weight cut-off bag or equivalent until the suspension conductivity is about 100 μS/cm. The suspension is then quantitatively transferred into centrifuge tubes and centrifuged at 2000 rpm for 30 min. The CNC supernatant is decanted and retained. The larger-sized cellulosic materials are washed with RO water and centrifuged at 2000 rpm for 15 min, followed by the collection of CNC suspensions. This cleaning step is repeated until clear supernatant is obtained and discarded. All CNC suspensions are mixed, and gravimetric analyses are performed on the solids content within the CNC suspensions and any unreacted materials to calculate the CNC and off spec yields.

2.4. CNC and CNC Reject Yield Calculations

CNC (materials in RO water suspensions) or CNC Reject (sediments) yield (%) was calculated using the following equation:

$$\text{Yield } (\%) = \frac{(M_2 - M_3) \times V_1}{M_1 \times V_2} \times 100\%$$

In this equation, M_1 represents the mass of pulp, M_2 is the total mass of oven-dried CNC (or CNC Reject) and container, M_3 is the mass of the container, V_1 is the total volume of prepared CNC (CNC Reject) suspension, and V_2 is the volume of CNC (or CNC Reject) suspension for oven-drying. Oven-drying is carried out at 105 °C to constant weight.

2.5. Dynamic Light Scattering (DLS)

DLS was used to determine CNC samples' particle size distribution and average particle size. Prior to analysis, 0.1 wt% colloidal suspensions of CNC were prepared by dispersing appropriate amounts of CNC materials in RO water followed by sonication for 3 min in a water bath (Sonicator bath, BRANSON 5510) at 20 °C. After equilibrating CNC suspensions (0.1 wt%) at room temperature for ~5 min, suspensions were placed in a temperature-regulated cell at 25.0 ± 0.1 °C. DLS measurements were conducted using a Malvern Zeta sizer Nano Series ZS instrument working at a 173° scattering angle. This instrument has a 4.0 mW He-Ne laser (λ = 633 nm) and an Avalanche photodiode detector. Size distributions were calculated using an inverse Laplace transform algorithm, and the hydrodynamic radii were calculated using the Stokes–Einstein equation.

2.6. Zeta Potential (ZP) Measurements

ZP is used to quantify the magnitude of electrical charge on the surface of CNC dispersed particles, which relates to the stability of CNC colloidal suspensions. ZP surface charges were evaluated using the Malvern Zeta sizer Nano Series ZS instrument. CNC

suspensions used in the ZP analysis were the same as the ones for DLS. The pH of CNC suspensions was approximately 6.5–7.

2.7. Conductometric Titration

The conductometric titration was performed with auto-titrator instruments (856 Conductivity module and 905 Titrando, Metrohm) available at InnoTech Alberta. This technique was used to determine sulfate half-ester contents of CNC materials. Before titration, CNC suspensions were first dialyzed using MilliQ water to remove any sulfur-containing and other ionic contaminants in the aqueous CNC suspension. The process continued until the conductivity of the suspension was around 50 μS/cm. After that, the CNC suspension was treated with a strong acid hydrogen exchange resin to ensure that sulfate half-ester groups are in the acidic form and thus detectable by titration with sodium hydroxide. The latter can then be used to titrate the CNC in acidic form and the sulfate half-ester content can be determined. This protocol was already approved by the Versailles Project on Advanced Materials and Standards (VAMAS) and provided to InnoTech Alberta for participating in the VAMAS inter-laboratory comparison (ILC) for CNC. The ILC activities aim to validate the proposed standard test methods in the context of the Canadian Standard Association technical committee (CSA TC) rules. The detailed protocol (VAMAS TWA-34) for measuring the sulfate half-ester contents in cellulose nanocrystals by conductometric titration is available for consultation if required. They cannot be disclosed due to confidentiality.

2.8. Rheological Measurements

The viscosity measurements of 1 wt% CNC suspensions were performed using an AR G2 TA Instruments rheometer. A cone-and-plate geometry was used, which allows for low sample volume and accurate rotation generation. The cone is a 60 mm aluminum cone with a 1° angle, suitable for low to medium viscosity fluids. The gap was set at 56 μm. The viscosity of the suspensions was measured against shear rates from 0.1–1000 s^{-1}.

2.9. Pulp Viscosity Measurements

The viscosity measurements of all pulp samples were determined using a capillary viscometer according to the TAPPI Standard Methods T230 om-19 (2013).

2.10. Thermogravimetric Analysis (TGA)

The thermal resistance analysis was carried out under a nitrogen atmosphere using a TGA model Q500 thermogravimetric analyzer. The weight of samples varied from 6 to 10 mg and from 10 to 15 mg for the pulp and CNC samples, respectively. The temperature was increased from 30 °C to 600 °C at heating of 10 °C/min. The nitrogen gas flow rate was 60 mL/min. All pulps were in a dry state, while the CNC suspensions were freeze-dried before thermal resistance evaluation.

2.11. Scanning Electron Microscopy (SEM)

The morphologies of the freeze-dried CNC materials prepared with untreated and oxidized feedstocks from both HW and SW were investigated by SEM using a Hitachi model S-4800 apparatus equipped with a field emission source. The SEM was operated at a voltage of 1 kV.

3. Results

3.1. Oxidation of SW and HW Kraft Pulps

In this study, fully bleached softwood (SW) and hardwood (HW) pulps with chemical composition profiles, as reported in Table 1, were oxidized under three different conditions using oxygen (O_2) oxidation methods. Initially, high consistency (20–28%), medium consistency (10–14%), and low consistency (3–5%) oxygen conditions were considered. However, due to the limitation of the operating apparatus, which could not operate at 20–28% consistency, low (4%), medium (10%), and high-end of medium consistency (14%)

were utilized to oxidize pulps. The details of oxidation reaction conditions are reported in Table 2.

Table 1. Chemical compositions of SW and HW chemical kraft pulps.

Sample Name	Solid Content, %	α-Cellulose, %	Acid Insoluble Lignin, %	Ash, %	Acetone Extractive, %
SW	97.30	84.4	3.87	0.50	0.069
HW	96.87	92.5	1.83	0.56	0.356

Table 2. The conditions for oxidation of fully bleached pulps by Parr reactor.

Sample	Pulp, g OD	NaOH, %	Consistency, %	Temp., °C	O_2, psi	Time, min
HW1	100	1.0	4	85	80	50
HW2	100	2.0	10	105	90	60
HW3	100	3.0	14	115	100	90
SW1	100	1.0	4	85	80	50
SW2	100	2.0	10	105	90	60
SW3	100	3.0	14	115	100	90

Temp.: Temperature, OD: Oven-Dry.

The reactions of carbohydrates under oxygen delignification conditions have been reviewed by Sjöström [14]. Generally, the reactions can be divided into two categories—those attacking glycosidic linked units and those attacking terminal reducing sugar units. The latter reaction can be both stabilizing and degrading [15].

Reactions of the first type cause or initiate depolymerization, which can lead to a drop-in viscosity and weakening of the mechanical strength of fibres. It diminishes pulp yield during oxygen pulping and bleaching if not adequately controlled.

Reactions of the second type can cause modifications of sugar units from the reducing-end of polysaccharides, causing either alkali stabilization by acid end-units, which is important and characteristic for oxygen-alkali oxidation, or peeling, which results in low-molecular-weight acid.

Although both reactions are associated with carbohydrate degradation, the first type (random chain cleavage) is more significant since it has a greater impact on cellulose chain breakage leading to a lower average length of cellulose. In addition, transition metals such as iron, manganese, and copper, when found in small quantities in unbleached pulps, promote carbohydrate degradation.

Several studies [14,15] proposed that the rate-determining step during glycosidic degradation is the hydrogen abstraction from a carbon atom of an ionized or un-ionized sugar hydroxyl group. The oxidation of this group to their corresponding carbonyl group and its position on the glycosidic units play an important role in determining the oxidation pathway of these cyclic sugar rings. The oxidation of carbohydrates may lead to degradation of the cellulosic chain by a β-elimination mechanism or may not cause chain cleavage but instead results in the formation of acidic products. As illustrated in Figure 2, most of these newly formed compounds bear at least one carboxylate group. Amongst a variety of these compounds, furanosidic glucoside is the most dominant product formed from the diketo compound by a benzilic acid type of rearrangement.

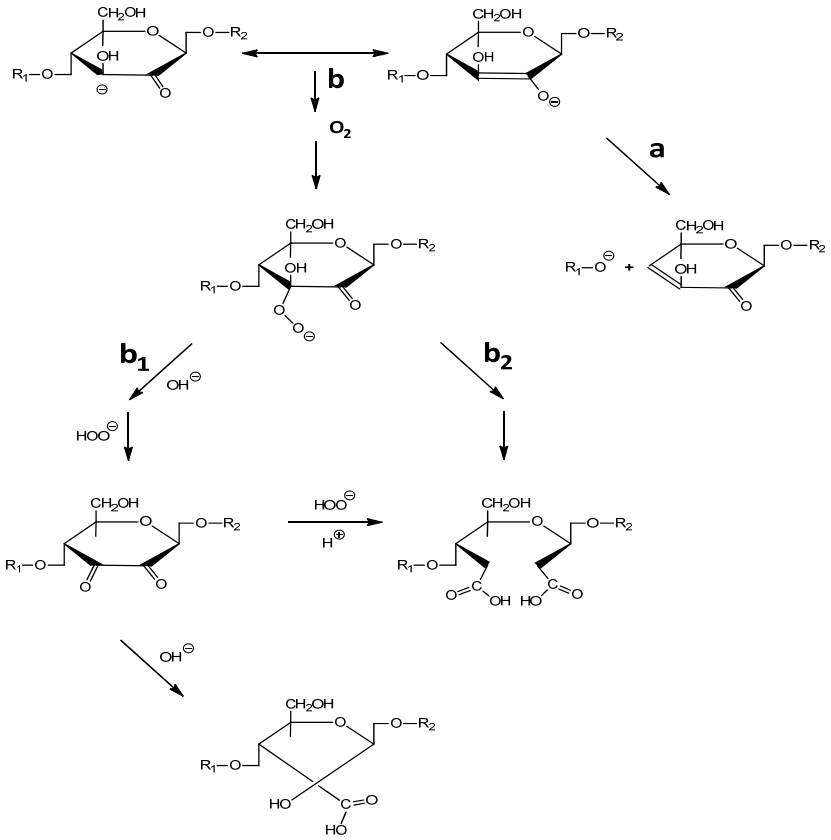

Figure 2. Oxidation of the cellulose chain and its products under O_2-alkali.

The effect of oxygen oxidation on the pulp viscosity for HW and SW was measured under different consistencies and compared to the starting materials. The detailed information is reported in Table 3 and illustrated in Figure 3.

The experimental data show the pulp DP dropped as the consistency increased from 4% to 14%. The DP for SW pulp was recorded to be lower than the HW pulp.

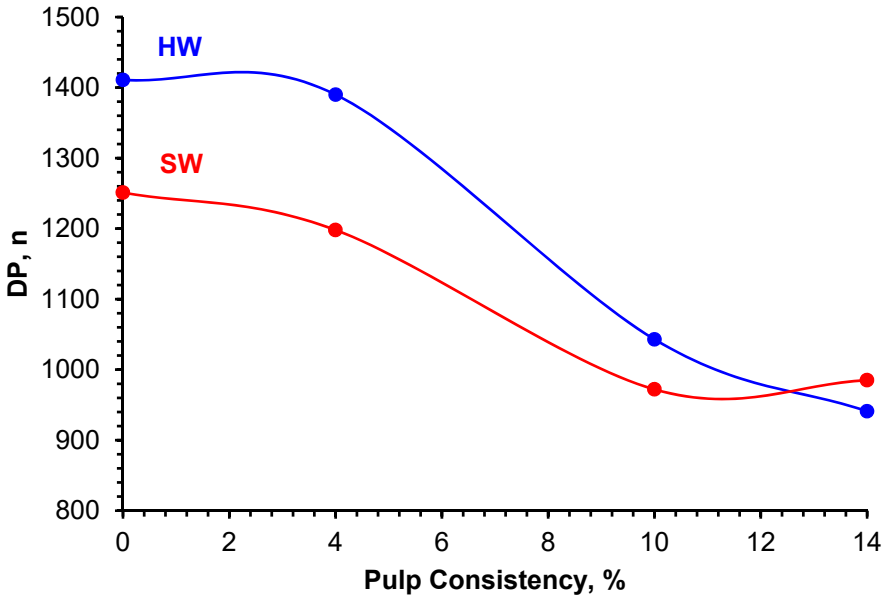

Figure 3. The effect of oxidation on the DP of HW and SW pulps.

Table 3. Determination of the degree of polymerization (DP) for oxidized pulps.

Sample	Consistency, %	DP, *n*
HW Control	0	1411
HW1	4	1390
HW2	10	1043
HW3	14	941
SW Control	0	1251
SW1	4	1198
SW2	10	972
SW3	14	985

3.2. CNC Preparation

The oxidized pulp samples were subsequently subjected to acid hydrolysis for the preparation of CNC under conventional conditions. The CNC was prepared at 63.5% sulfuric acid, 45 °C, 120 min, with an 11.3:1 acid-to-pulp ratio under 200 rpm.

For the CNC and reject yields calculations, each neutralized sample was dialyzed to bring its conductivity to about 100 μS/cm and then centrifuged to separate its content into its corresponding CNC and reject materials. After that, known amounts of suspensions were oven-dried for yield determination. The corresponding CNC and reject yields for each purified sample are reported in Table 4. Data show that the yields of CNC from oxidized HW and SW pulps were higher than those from HW Control and SW Control. For example, the yields of CNC from oxidized HW pulps are in the 18.2 and 21.4% range compared to 13.4% for CNC-HW Control. The corresponding yields for the CNC from oxidized SW pulps are 19.1 and 23.1%, compared to 17.3% for CNC-SW Control. Generally, data show that the oxidation promoted the increase of the CNC production yields regardless of the pulp's source and grade. In all cases, lower than 10% reject yields were obtained.

Table 4. Determination of CNC and reject yields from control and oxidized HW and SW pulps.

Sample	Yield, %	
	CNC	Reject
CNC-HW Control	13.4	3.1
CNC-HW1	18.9	7.4
CNC-HW2	20.4	5.1
CNC-HW3	21.4	5.1
CNC-SW Control	17.3	4.7
CNC-SW1	19.1	3.2
CNC-SW2	19.9	3.2
CNC-SW3	23.1	1.6

Conditions for CNC production: 63.5 wt% H_2SO_4, 45 °C, 120 min, 11.3:1 acid-to-pulp ratio, 200 rpm.

The particle size distribution (PSD) of CNC suspensions derived from control and oxidized HW and SW pulps were analyzed by DLS. At the same time, their surface charges and colloidal stability were evaluated by Zeta Potential (ZP) measurements. Data presented in Table 5 confirmed the presence of negative charges ("negative ZP values") on the CNC surface and the stability of resulting CNC suspensions (ZP values < -31 mV) in all cases.

DLS data show average particle sizes (PS) in the range of 116 and 383 nm for CNC suspensions prepared using control and oxidized HW pulps. Especially, CNC-HW2 showed bimodal average particles size of 116 and 383 nm. The lowest average PS was obtained with CNC-HW Control. Overall, the data also show that the average particle sizes of CNC prepared from oxidized HW pulps are larger than the ones prepared from HW Control. In Table 5, the polydispersity index (PDI), a dimensionless measure of the broadness of the size distribution, was found to be in the 0.436 and 0.723 range for CNC from oxidized

HW pulps as compared to 0.397 for CNC from HW Control. This indicates that CNC from oxidized HW pulps has broad PSD and contains larger particles. In Table 5, data show that CNC suspensions prepared from SW Control and oxidized SW pulps displayed average particle sizes in the 102 and 173 nm range. The lowest value of average PS was obtained with CNC-SW Control. The PDI of CNC from oxidized SW pulps was found to be in the 0.437 and 0.570 range compared to 0.424 for CNC-SW Control. This PDI range for CNC from oxidized SW pulps also indicates that these samples have broad PSD and contain larger particles. The latter shows that the level of oxidation slightly impacted the PSD of the CNC SW samples series. According to DLS data, CNC materials from the SW pulps series seem to behave differently than those from the HW pulps series.

Table 5. Analysis of never-dried CNC suspensions from control and oxidized HW and SW by DLS and ZP at pH 6.5.

Sample	DLS		Zeta Pot., mV
	d_{av}, nm	PDI	
CNC-HW Control	116.8 ± 4.4	0.397 ± 0.017	−45.4 ± 1.3
CNC-HW1	137.8 ± 4.3	0.453 ± 0.017	−45.4 ± 0.8
CNC-HW2	116.4 ± 10.4/383.1 ± 5.7	0.723 ± 0.030	−52.2 ± 0.2
CNC-HW3	130.8 ± 6.4	0.436 ± 0.008	−46.3 ± 2.4
CNC-SW Control	102.4 ± 22.6	0.424 ± 0.026	−43.5 ± 1.2
CNC-SW1	120.8 ± 7.3	0.465 ± 0.016	−46.2 ± 0.4
CNC-SW2	112.7 ± 6.3	0.437 ± 0.008	−54.3 ± 0.1
CNC-SW3	173.6 ± 3.5	0.570 ± 0.037	−51.7 ± 0.8

DLS: Dynamic Light Scattering (d_{av}: average particle size)/Zeta Pot.: Zeta potential. PDI: Polydispersity Index.

Conductometric titration was performed to determine the sulfate half-ester contents of CNC materials. This method is more accurate than elemental analysis (EA) by combustion (CHNS). The latter considers the total sulfur content, meaning all sulfate groups attached to the CNC surface and as impurities. At the same time, the conductometric titration involved a highly purified CNC suspension (removal of traces by dialysis). Data in Table 6 and graphs in Figure 4 show that the sulfate half-ester contents of all HW and SW-derived CNC materials fall between 313 and 369 mmol/kg. The highest sulfate half-ester contents were obtained with CNC-HW Control and CNC-SW Control as compared to the ones for CNC from oxidized HW and SW pulps where changes in contents were not substantial. This may indicate that the oxidation level was insufficient to impact the surface charge density. Still, the oxidation process seems to demonstrate the control of the sulfate half-ester contents on the CNC surface.

Table 6. Total sulfur and sulfate half-ester contents on different CNC surfaces.

Sample	Conductometric Titration, mmol/kg
CNC-HW Control	356.47
CNC-HW1	335.20
CNC-HW2	313.30
CNC-HW3	329.05
CNC-SW Control	368.30
CNC-SW1	340.52
CNC-SW2	340.45
CNC-SW3	320.78

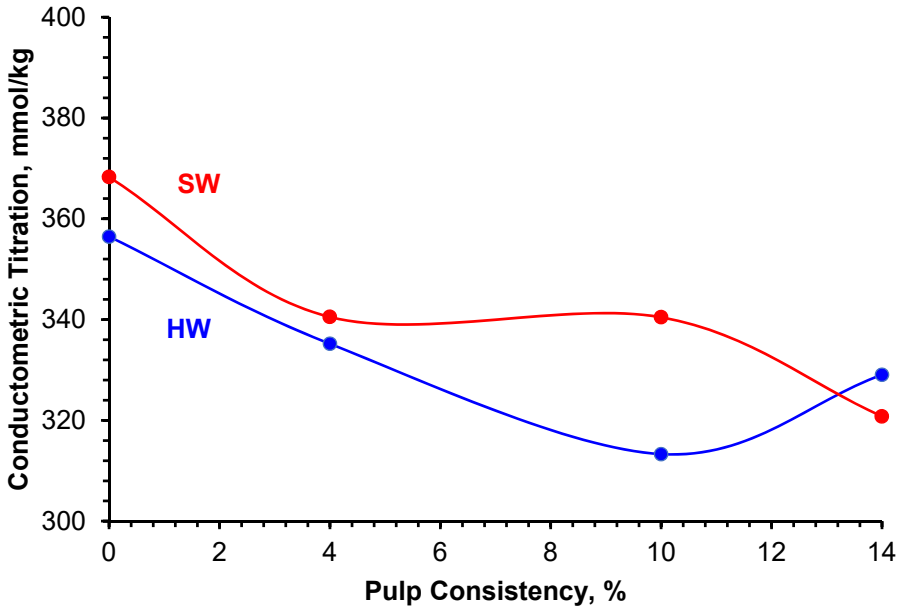

Figure 4. Effect of oxidation on the sulfate half ester content on HW and SW derived CNC by conductometric titration.

3.3. Thermogravimetric Analysis (TGA)

This test method allows the assessment of dry material (untreated and oxidized pulps, derived CNC, etc.) thermal stability through the determination of the temperature at which the material starts to decompose and may also provide an indication of usability for high-temperature processing and end-use.

The thermal properties of control and oxidized HW and SW pulps and their derived CNC samples were evaluated using TGA under a nitrogen atmosphere. The resulting data are reported in Tables 7 and 8, while Figures 5 and 6 show their thermogravimetric (TGA) and differential gravimetric (DTG) curves.

Generally, the degradation profile of pulps and CNC by TGA is divided into three stages.

First stage: all samples displayed a small weight loss in the 30–150 °C temperature range, as shown in Figures 5 and 6. This loss is associated with the evaporation of the moisture contained in the pulp and CNC samples and is in the 3 to 4.5% range, as reported in Tables 7 and 8. A plateau follows this loss until the initial degradation temperature (T_{iD}), as reported in Tables 7 and 8 and shown in Figures 5 and 6 for each sample (pulp or CNC), is reached. The T_{iD} of HW Control and SW Control, as well as their oxidized derivatives, were about 275 °C and were higher than the T_{iD} of their corresponding CNC materials because of the absence of sulfate groups on the pulps' surface. In addition, in Table 7, the number of residues from oxidized HW pulps decreases with increased consistency (percentage of oxidation) but stays lower as compared to the HW Control. The trend is as follows: 6.8 wt% (HW Control, 0%) > 6.3 wt% (HW1, 4%) > 4.2 wt% (HW2, 10%) > 2.7 wt% (HW3, 14%). On the contrary, it was found that the number of residues from oxidized SW pulps increases with increased consistency and stays higher compared to the SW Control. The trend is as follows: 8.1 wt% (SW1, 4%) > 8.0 wt% (SW3, 14%) > 6.8 wt% (SW2, 10%) > 5.5 wt% (SW Control, 0%).

Second stage: the degradation of cellulose usually occurs after the plateau in the 250 °C and 400 °C temperature range [16]. The latter is affected by the level of purity of the cellulose. For instance, the presence of sulfate groups on the CNC surface will lower their T_{iD} as compared to the ones of their pure cellulose-based precursors. This is validated by data reported in Tables 7 and 8 for all CNC materials. Again, the higher the density of sulfate groups on the CNC surface, the lower the T_{iD} will be. TGA and DTG curves in Figures 5 and 6 show that the T_{iD} range of pure cellulose shifted from 250–400 °C

to 200–315 °C due to the presence of sulfate groups on the CNC materials surface. In these ranges, the primary pyrolysis of cellulose is catalyzed by sulfate groups onto CNC materials surface. The presence of sulfate groups on the CNC surface was confirmed by conductometric titration data in Table 6 and zeta potential (ZP) measurements in Table 5. The effect of impurities on the T_{iD} of any CNC material may also be revealed by the level of residue generated after TGA. For example, CNC from oxidized HW pulps displayed residues in the 20.6 and 27.2% range, compared to 29.5% for the CNC-HW Control. That may explain the higher T_{iD} of CNC materials from oxidized HW pulps compared to the CNC-HW Control. The T_{iD} for CNC from oxidized HW pulps was in the 235–240 °C range compared to 220 °C for HW-CNC Control.

In contrast, CNC from oxidized SW pulps displayed residues in the 23.1 and 26.4% range, compared to 21.9% for the CNC-SW Control. Therefore, the T_{iD} of the CNC from oxidized SW pulps was lower than that of CNC-SW Control. The T_{iD} for CNC from oxidized SW pulps was in the 205–210 °C range compared to 220 °C for CNC-SW Control. In all cases, the T_{iD} of the resulting CNC materials was out of the 250–275 °C range for current CNC materials. These lower T_{iD} values, as reported in Table 8, may also originate from either the severity of the reaction conditions as revealed by the high levels of sulfate half-ester contents of HW and SW CNC-derived samples or the generation of new types of CNC materials.

Table 7. Summary of TGA data of untreated and oxidized HW and SW pulps.

Sample	Consistency, %	M.C. at 150 °C, %	$T_{5\%}$, °C	$T_{50\%}$, °C	T_{max}, °C	Residue at 600 °C, %	T_{iD}, °C
					1		
HW Control	0	3.4	273.6	340.7	344.8	6.8	275.0
HW1	4	3.1	272.0	344.4	348.8	6.3	275.0
HW2	10	3.0	276.8	346.0	350.4	4.2	275.0
HW3	14	3.0	281.6	343.2	348.0	2.7	275.0
SW Control	0	3.5	271.2	347.0	352.0	5.5	275.0
SW1	4	3.5	264.8	346.2	351.0	8.1	275.0
SW2	10	3.4	263.2	346.4	350.4	6.8	275.0
SW3	14	3.4	264.0	346.5	350.4	8.0	275.0

$T_{5\%}$: Temperature of 5% weight loss. M.C.: Moisture content at 150 °C. $T_{50\%}$: Temperature of 50% weight loss. T_{max}: Temperature of maximum weight loss. T_{iD}: initial decomposition or degradation temperature. Residue: material left after pyrolysis at around 600 °C.

Table 8. Summary of TGA data of CNC samples.

Sample	M.C. at 150 °C, %	$T_{5\%}$, °C	$T_{50\%}$, °C	T_{max}, °C		Residue at 600 °C, %	T_{iD}, °C
				1	2		
CNC-HW Control	3.7	225.6	336.0	244.0	284.8	29.5	220.0
CNC-HW1	3.8	241.4	318.6	n/a	285.6	20.6	235.0
CNC-HW2	4.3	239.0	338.6	259.2	285.1	23.8	235.0
CNC-HW3	3.8	247.5	315.0	n/a	286.4	27.2	240.0
CNC-SW Control	4.5	217.6	329.0	n/a	284.8	21.9	220.0
CNC-SW1	4.0	216.8	343.1	240.0	284.0	25.7	205.0
CNC-SW2	4.2	211.2	343.2	239.2	283.2	26.4	205.0
CNC-SW3	4.4	212.0	333.6	242.4	284.8	23.1	210.0

$T_{5\%}$: Temperature of 5% weight loss. M.C.: Moisture content at 150 °C; $T_{50\%}$: Temperature of 50% weight loss. T_{max}: Temperature of maximum weight loss. T_{iD}: initial decomposition or degradation temperature. Residue: material left after pyrolysis at around 600 °C. n/a: non-applicable.

Third and last stage: pyrolysis of hydrocarbon chains occurs along with the slow charring process of the solid residue [17,18] and corresponds to 400–600 °C temperature range for pulps (control and oxidized) and 315–600 °C temperature range for their derived CNC materials.

The DTG data in Table 7 and curves in Figure 5 show that the maximum decomposition temperatures (T_{max}) positions of oxidized HW pulps were almost the same (~348–350 °C) and slightly higher than the HW Control (344 °C). For their corresponding CNC, as shown in Table 8 and Figure 6, the T_{max} positions were almost the same (~285–286 °C). For the SW pulps series, data in Table 7 and DTG curves in Figure 5 show that the T_{max} positions for oxidized SW pulps were almost the same (350–351 °C) and slightly higher than the SW Control (352 °C). This observation indicates that the oxidation process and its level do not affect the T_{max} position of the SW pulps series.

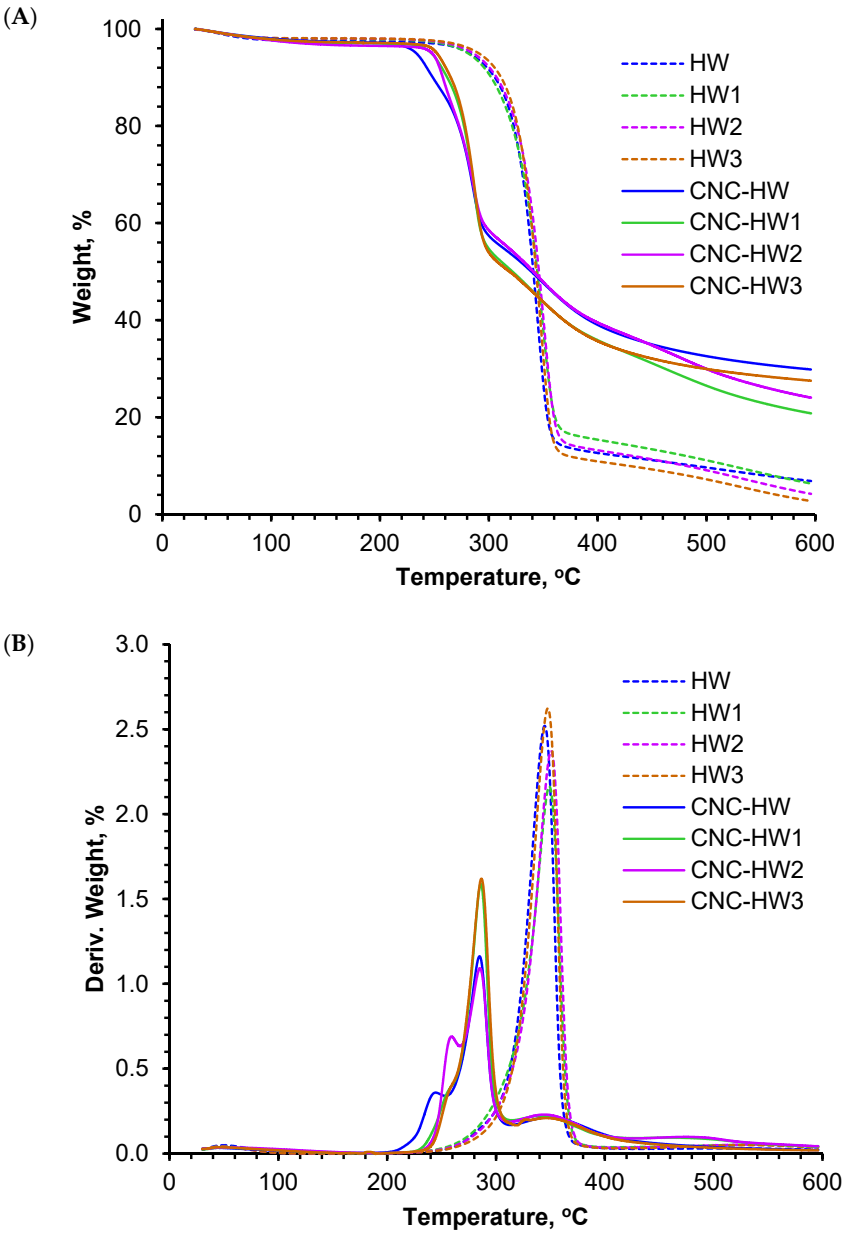

Figure 5. TGA (**A**) and DTG (**B**) curves of HW Control and oxidized HW and their corresponding CNC.

Generally, the DTG curves for CNC materials show one (one T_{max}) only in the 250 and 325 °C temperature range. This range may be affected by the hydrolysis reaction conditions and the pulp quality. This is the case for CNC-HW1 and CNC-HW3 in Figure 6, where the T_{max} positions were around 286 °C and in the 220 and 315 °C temperature range. CNC-HW2 and CNC-HW Control samples also displayed T_{max} positions at about 286 °C

with two short T_{max} positions (shoulders) at 259 and 244 °C, respectively, as reported in Table 8 and shown in Figure 6.

For the CNC-SW samples series, the DTG curves show that the T_{max} also fell in the 200–315 °C temperature range, which may also be due to the high density of sulfate groups on the CNC materials surface. One peak with a position around 285 °C was observed for CNC-SW Control. At the same time, each CNC sample from the oxidized SW pulps series (CNC-SW1, CNC-SW2 or CNC-SW3) displayed two maximum decomposition peaks (one minimum and one maximum). The minima and maxima were around 240 °C and 285 °C, respectively.

Overall, the DTG curves for CNC samples in Figure 6 show two or multiple maximum decomposition temperatures in the 200 and 315 °C temperature range, indicating that several specimens have been decomposed in this temperature range. In addition, the initial decomposition temperatures (T_{iD}) for the CNC-SW samples series were lower than the ones of the CNC-HW samples series. This may be due to the lower DP of SW pulps series, which probably allows them to break down into smaller sizes of CNC materials.

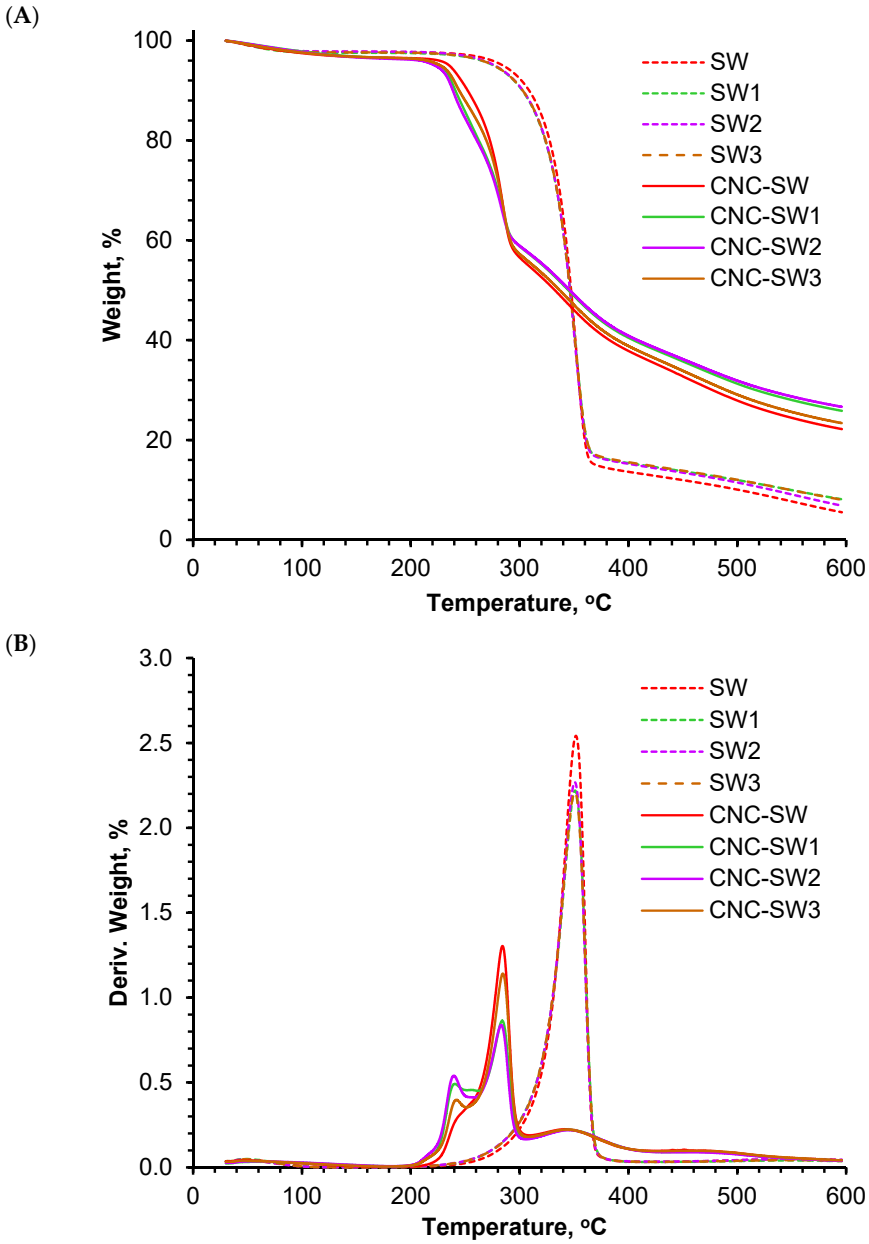

Figure 6. TGA (**A**) and DTG (**B**) curves of SW Control and oxidized SW and their corresponding CNC.

3.4. Rheological Measurements

The viscosities of the CNC suspensions prepared with untreated and oxidized feedstocks from both HW and SW were evaluated and presented in Figures 7 and 8. The emerging data show that within the same feedstock, the pulp oxidation conditions somehow affect the viscosity of the CNC suspensions. The viscosities of the CNC suspensions prepared from pulps after oxidation under conditions 1 and 2 are higher than the control, and the viscosities of the CNC suspensions prepared from pulps after oxidation under condition 3 are lower as compared to the control. This behavior appears in the same manner for CNC prepared from HW and SW. From the results obtained, the orders of viscosities for the CNC suspensions prepared from the untreated and oxidized pulps can be arranged as CNC-HW1 > CNC-HW2 > CNC-HW Control > CNC-HW3 and CNC-SW1 > CNC-SW2 > CNC-SW Control > CNC-SW3.

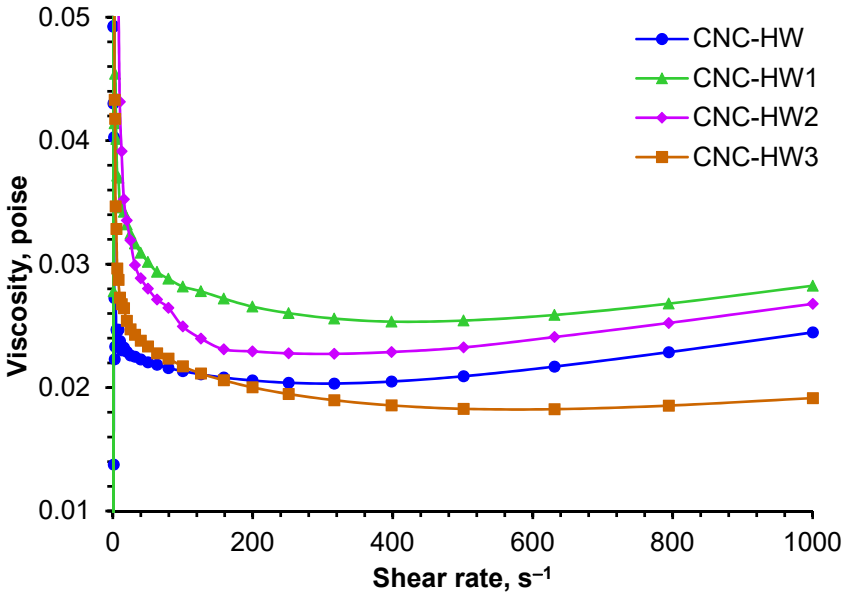

Figure 7. Viscosity measurements of CNC from HW and oxidized HW.

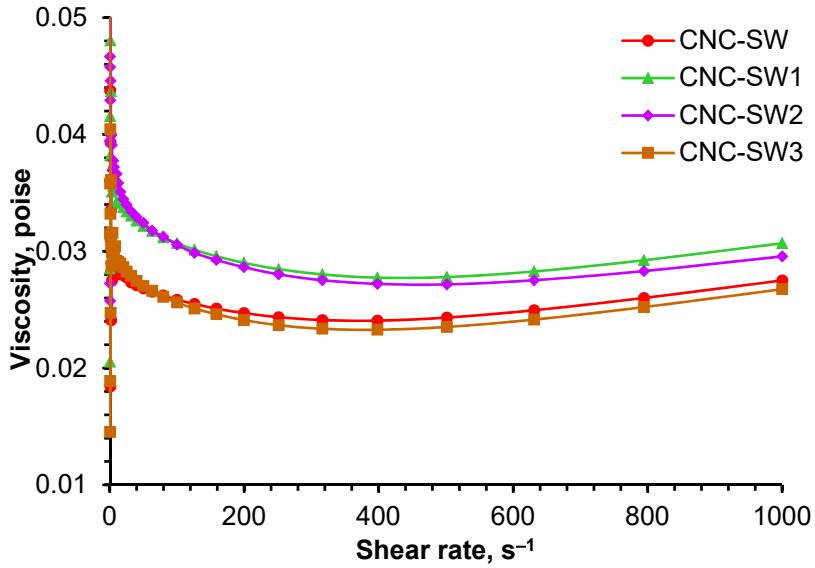

Figure 8. Viscosity measurements of CNC from SW and oxidized SW.

Comparing CNC prepared from HW and SW pulps, the results demonstrate that the viscosity of CNC suspension prepared from SW Control is higher than that of CNC

suspension prepared from HW Control. This phenomenon appears similarly for the CNC suspensions prepared from the oxidized pulps under the same oxidized conditions (CNC-HW1 vs. CNC-SW1, CNC-HW2 vs. CNC-SW2, and CNC-HW3 vs. CNC-SW3) as presented in the appendix (Figures 9–12). This may be due to the longer fibre of the SW pulp as compared to HW pulp and the oxidized ones. In general, the rheological behavior of these CNC suspensions is a combination of non-Newtonian and Newtonian behaviors. At lower shear rates, they behave as non-Newtonian, but as the shear rate increases, they tend to exhibit a Newtonian behavior. This is caused by particles starting to untangle each other and begin aligning themselves in the flow direction as the shear rate increases.

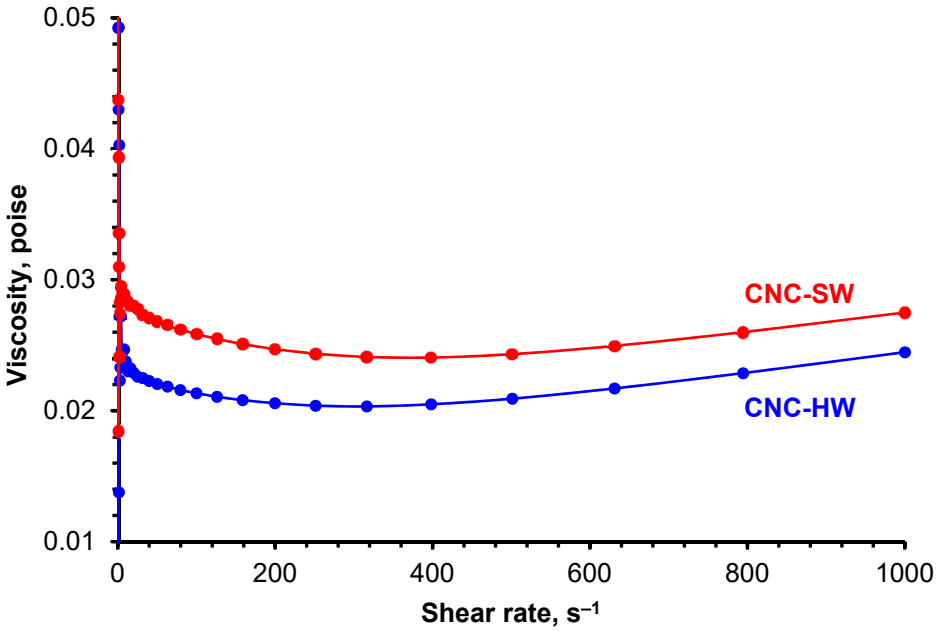

Figure 9. Viscosity compression of CNC from HW and SW.

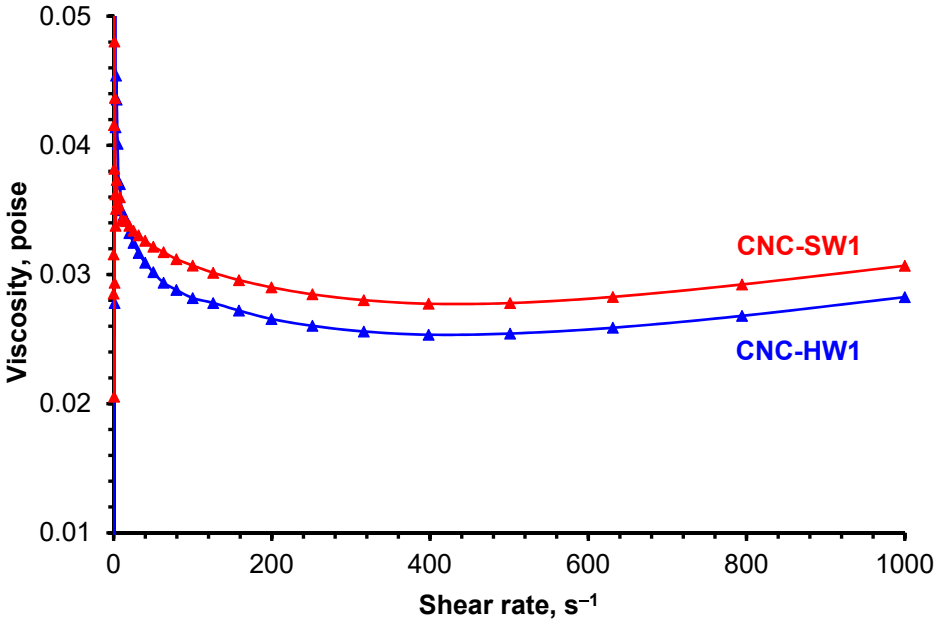

Figure 10. Viscosity comparison of CNC from oxidized HW1 and oxidized SW1.

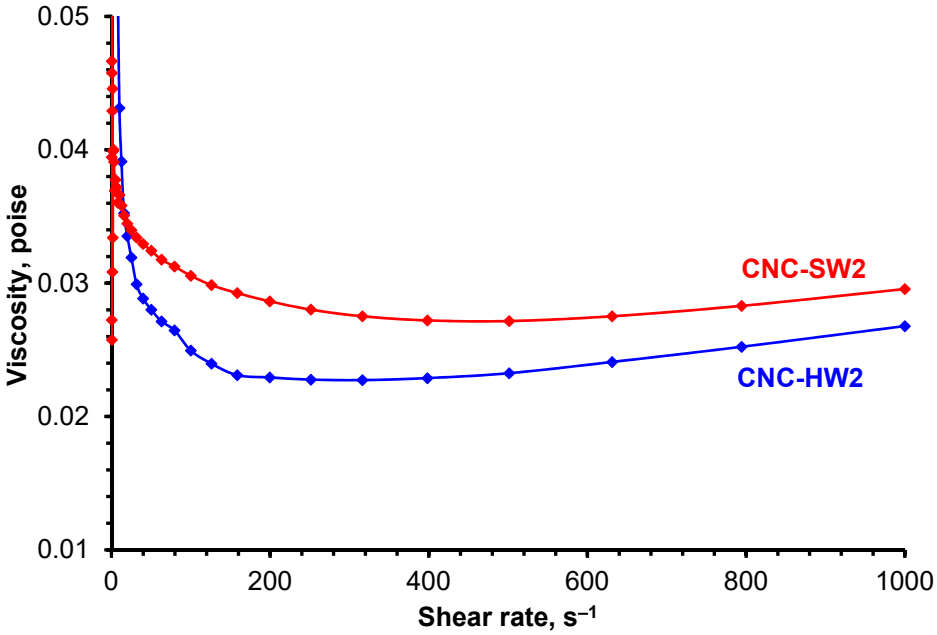

Figure 11. Viscosity comparison of CNC from oxidized HW2 and oxidized SW2.

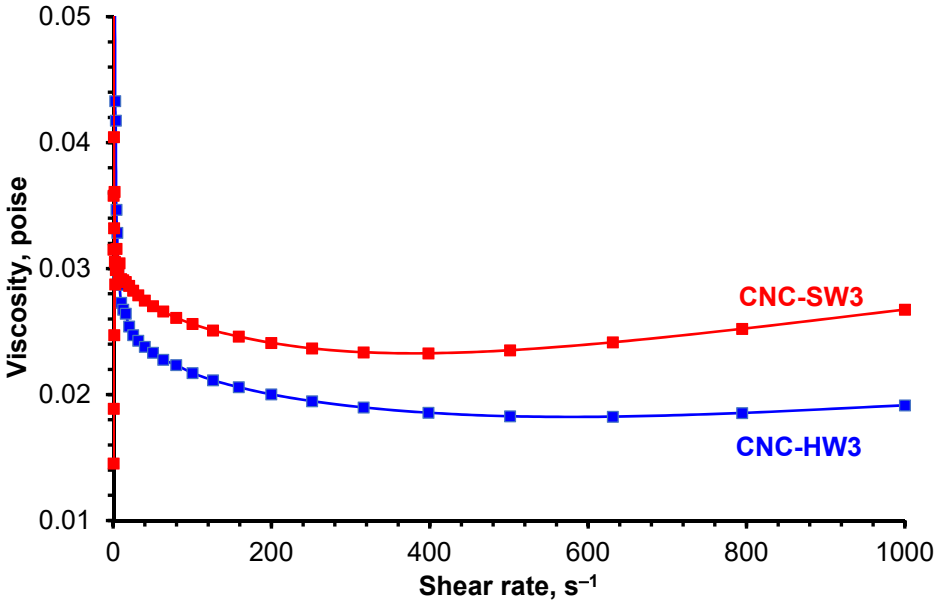

Figure 12. Viscosity comparison of CNC from oxidized HW3 and oxidized SW3.

3.5. Scanning Electron Microscopy (SEM)

The SEM images of the freeze-dried CNC prepared with untreated and oxidized feedstocks from both HW and SW were evaluated and presented in Figures 13 and 14. The SEM images show non-uniform and random flake-like structures for all cases. Therefore, the SEM images for freeze-dried CNC prepared with untreated and oxidized feedstocks from HW and SW did not show significant differences between sets of samples.

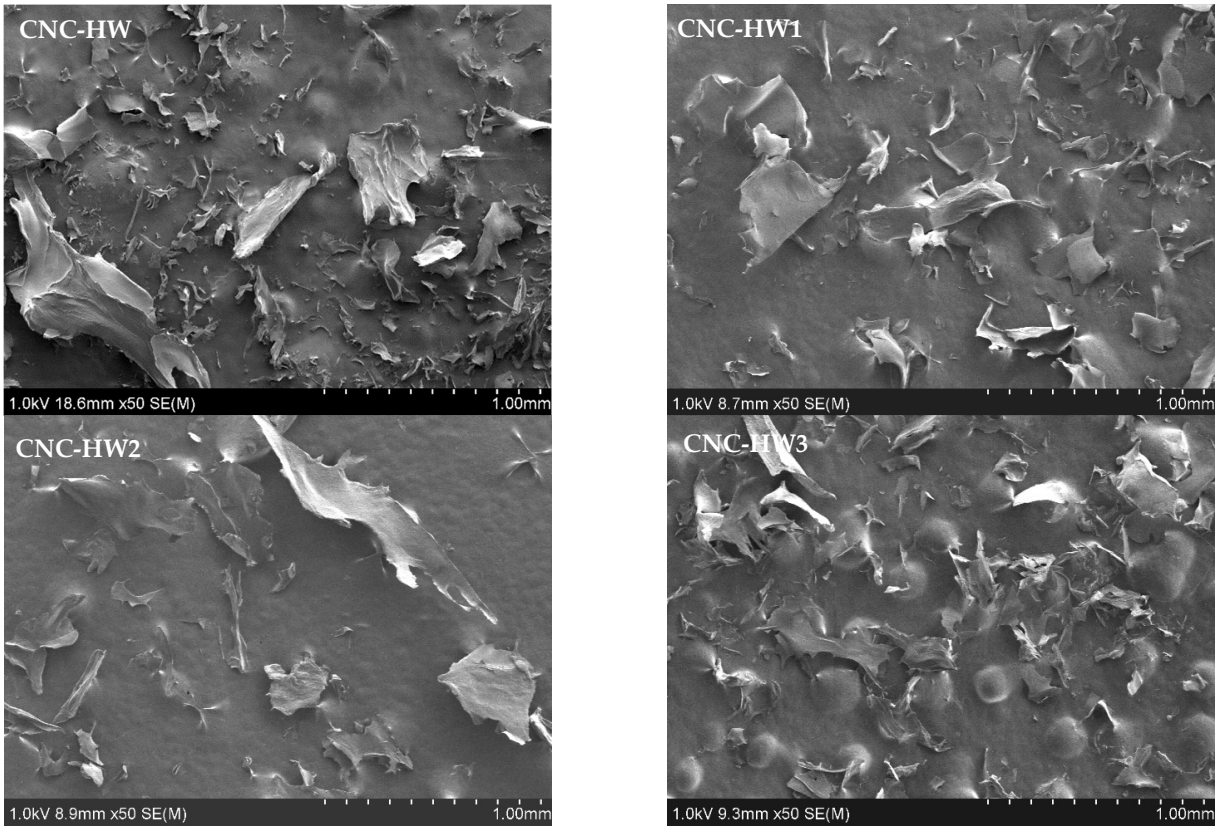

Figure 13. SEM images of CNC from HW and oxidized HW.

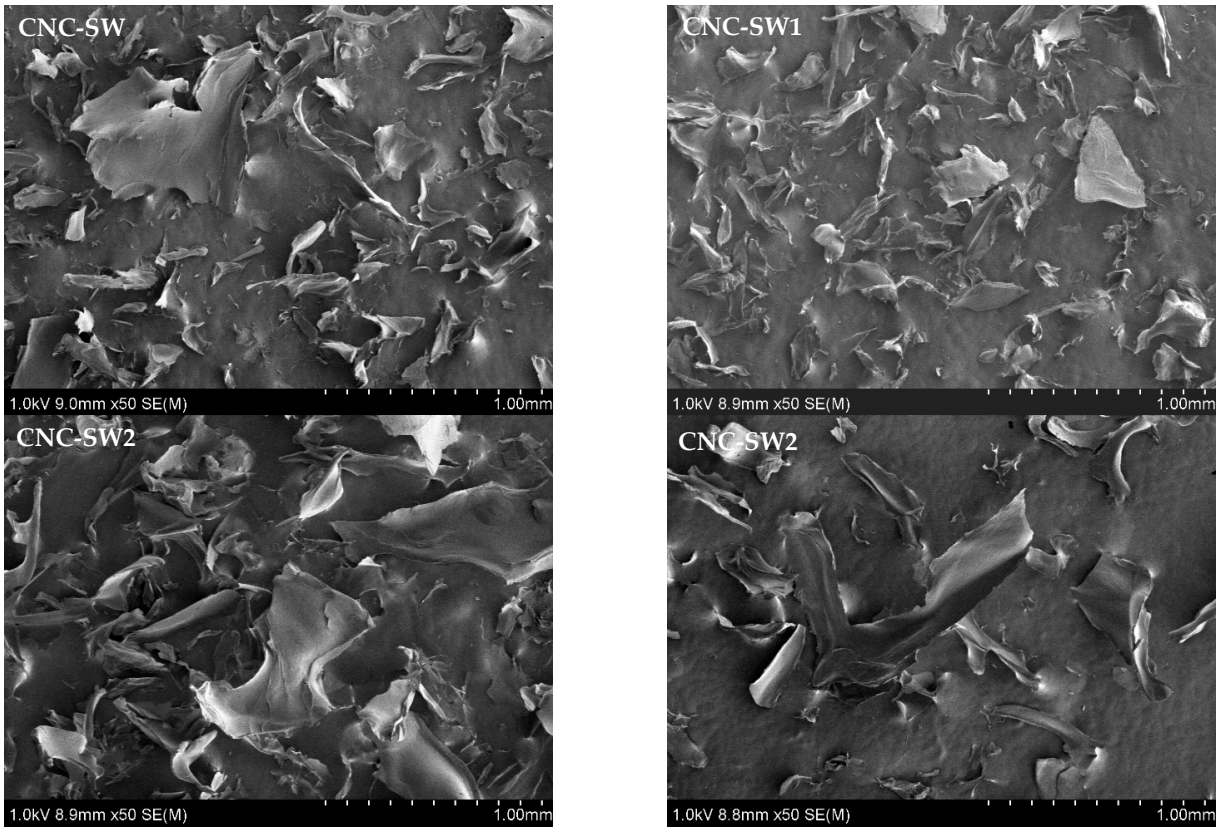

Figure 14. SEM images of CNC from SW and oxidized SW.

4. Conclusions

In this study, both bleached softwood (SW) and hardwood (HW) kraft pulps were oxidized using oxygen (O_2). The subsequent oxidized samples were hydrolyzed with concentrated sulfuric acid under a conventional procedure to produce CNC. The characterization of CNC materials has confirmed our hypothesis. The emerging data have shown that the SW has lower DP than HW under similar oxidation conditions. The pulp oxidation process helped improve the CNC yields compared to the controls. The CNC yield increased as the oxidation consistency increased from 4 to 14%. However, different oxidation consistencies of pulps did not affect the CNC suspension stability. The oxidation process reduced the sulfate half-ester contents compared to the controls. The sulfate half-ester contents for CNC-SW were higher than their CNC-HW counterparts. Pulp oxidation improves the thermal stability of CNC for HW more than SW pulps. The oxidation of SW and HW also affects the viscosity of CNC suspensions, which was consistently higher in SW than in HW pulp. The emerging data help to prepare and engineer CNC tailored to specific applications.

Author Contributions: B.A.: methodology, writing—review & editing; C.D.: investigation; T.-D.N.: investigation, writing—review & editing; Z.Z.: investigation; H.L.: investigation. All authors have read and agreed to the published version of the manuscript.

Funding: The authors express their appreciation to InnoTech Alberta's Program Investment for providing financial support for this project.

Institutional Review Board Statement: Not applicable.

Informed Consent Statement: Not applicable.

Data Availability Statement: Not applicable.

Acknowledgments: We extend our gratitude to all the scientists and InnoTech Alberta staff for providing technical support. We also gratefully acknowledge Kathy Gates and Hamdam Gaminian for preparing this manuscript and Brent Scorfield and Usukuma Ekuere for editing it.

Conflicts of Interest: The authors declare no conflict of interest.

References

1. De Souza Lima, M.M.; Borsali, R. Rodlike cellulose microcrystals: Structure, properties, and applications. *Macromol. Rapid Commun.* **2004**, *25*, 771–787. [CrossRef]
2. Huang, J.; Chang, P.R.; Dufresne, A. *Polysaccharide Nanocrystals: Current Status and Prospects in Material Science, Polysaccharide-Based Nanocrystals: Chemistry and Applications*, 1st ed.; Chemical Industry Press: Beijing, China; Wiley-VCH Verlag GmbH & Co. KGaA: Berlin, Germany, 2015; pp. 1–13.
3. Oksman, K.; Aitomaki, Y.; Mathew, A.P.; Siqueira, G.; Zhou, Q.; Butylina, S.; Tanpichai, S.; Zhou, X.; Hooshmand, S. Review of the recent developments in cellulose nanocomposite processing. *Compos. Part A* **2016**, *83*, 2–18. [CrossRef]
4. Dufresne, A. Cellulose nanomaterials as green nanoreinforcements for polymer nanocomposites. *Philos. Trans. R. Soc. A Math. Phys. Eng. Sci.* **2018**, *376*, 20170040. [CrossRef] [PubMed]
5. Mariano, M.; Kissi, N.; Dufresne, A. Cellulose nanocrystals and related nanocomposites: Review of some properties and challenges. *J. Polym. Sci.* **2014**, *52*, 791–806. [CrossRef]
6. Marchessault, R.H.; Morehead, F.F.; Koch, M.J. Some hydrodynamic properties of neutral suspensions of cellulose crystallites as related to size and shape. *J. Colloid Sci.* **1961**, *16*, 327–344. [CrossRef]
7. Candanedo, S.B.; Roman, M.; Gray, D.G. Effect of conditions on the properties and behavior of wood cellulose nanocrystal suspension. *Biomacromolecules* **2005**, *6*, 1048–1054. [CrossRef] [PubMed]
8. Ranby, B.G.; Banderet, A.; Sillén, L.G. Aqueous colloidal solutions of cellulose micelles. *Acta Chem. Scand.* **1949**, *3*, 649–650. [CrossRef]
9. Klemm, D.; Heublein, B.; Fink, H.-P.; Bohn, A. Cellulose: Fascinating biopolymer and sustainable raw material. *Angew. Chem. Int. Ed.* **2005**, *36*, 3358–3393. [CrossRef] [PubMed]
10. Dufresne, A. *Nanocellulose: From Nature to High-Performance Tailored Materials*; Walter de Gruyter GmbH & Co KG: Berlin, Germany; Boston, MA, USA, 2012.
11. Habibi, Y.; Lucia, L.A.; Rojas, O.J. Cellulose nanocrystals: Chemistry, self-assembly, and applications. *Chem. Rev.* **2010**, *110*, 3479–3500. [CrossRef] [PubMed]

12. Pérez, S.; Mazeau, K. Conformations, structures and morphologies of celluloses. In *Polysaccharides: Structural Diversity and Functional Versatility*; Dimitriu, S., Ed.; Marcel Dekker: New York, NY, USA, 2004; pp. 41–68.
13. Sarkanen, K.V.; Islam, A.; Anderson, C.D. Ozonation. In *Methods in Lignin Chemistry*; Lin, S.Y., Dence, C.W., Eds.; Springer: Berlin, Germany, 1992; pp. 387–406.
14. Sjöström, E. Behavior of Pulp Polysaccharides during Oxygen-Alkali Delignification. In *Chemistry of Delignification with Oxygen, Ozone, and Peroxide*; The University of Tokyo: Tokyo, Japan, 1980; pp. 61–77.
15. Gratzl, J.S. *Reaction of Polysaccharides and Lignins in Bleaching with Oxygen and Related Species*; Tappi Oxygen Delignification Symposium Notes; Tappi Press: Atlanta, GA, USA, 1990; pp. 1–8.
16. Randriamanantena, T.; Razafindramisa, F.L.; Ramanantsizehena, G.; Bernes, A.; Lacabane, C. Thermal behaviour of three woods of Madagascar by thermogravimetric analysis in inert atmosphere. In Proceedings of the Fourth High-Energy Physics International Conference, Antananarivo, Madagascar, 21–28 August 2009.
17. Ping-Sheng, L.; Qiang, C.; Xiang, L.; Bo, Y.; Shi-Shan, W.; Jian, S.; Si-Cong, L. Grafting of zwitterion from cellulose membranes via ATRP for improving blood compatibility. *Biomacromolecules* **2009**, *10*, 2809–2816.
18. Jie, Y.; Qunxing, X.; Xuefei, Z.; Hailiang, Z. Temperature-induced chiral nematic phase changes of suspensions of poly (N,N-dimethylaminoethyl methacrylate)-grafted cellulose nanocrystals. *Cellulose* **2009**, *16*, 989–997.